CSCE Annual Conference

Growing with youth – Croître avec les jeunes

Laval (Greater Montreal)

June 12 - 15, 2019

AN INITIAL COMPARISON OF THE PERFORMANCE OF HOOKED PLAIN AND DEFORMED BARS

Vors, Bjorn[1], Feldman, Lisa R.[2,3]

[1]M.Sc. Student, Department of Civil, Geological, & Environmental Engineering, University of Saskatchewan, Canada

[2]Associate Professor, Department of Civil, Geological, & Environmental Engineering, University of Saskatchewan, Canada

[3]lisa.feldman@usask.ca

Abstract: A preliminary investigation of beam-column specimens containing 90 or 180°, 25 mm diameter plain round or modern deformed hooked bars were tested to establish the performance of hooked plain bars in comparison to hooked deformed bars. All specimens were designed to fail by anchorage of the hooked bars prior to bar yielding. It was determined that the anchorage capacity of 90 and 180° hooks for either bar type were similar; however, the anchorage capacity of the plain bars was about 30% less than that measured for the modern deformed bars. Slip of the hooked modern deformed bars also exceeded that of the hooked plain bars at both the normalized maximum and residual load levels.

1 INTRODUCTION

Provisions for calculating the development length of plain hooked bars were not included in historical versions of CSA A23.3 “Design of Concrete Structures” or ACI318 “Building Code Requirements for Structural Concrete.” Nonetheless, situations are encountered in practice where the capacity of such bars are required for the proper assessment of historical structures. Further, a literature review revealed the existence of only two studies (Mylrea 1924, Cleland 2001) that evaluated plain hooked bars, but neither of these provided direct information related to their capacity.

In contrast, provisions for hooked deformed bars as included in ACI318-14 (ACI318 2014) are based on a limited number of tests performed in the 1970s (Minor & Jirsa 1975, Marques & Jirsa 1975, Pinc et al. 1977). More recent works (Sperry et al. 2017a, 2017b, 2018) have provided a significant expansion of the test database, extending the range of concrete compressive strengths and yield strengths of the reinforcement, in addition to evaluating hook geometry (i.e. 90 and 180° hooks), bar size, side cover, bar position within the reinforcing cage, spacing between the hooked bars, degree of confining reinforcement, and embedment length. Changes to the provisions for the development length of deformed hooked bars have resulted and will be introduced in the 2019 edition of the ACI318 code.

Plain reinforcing bars do not include any deformations and so are unable to resist bond forces by mechanical interlock. Instead, bond is transferred exclusively by adhesion between the bar and the surrounding concrete, and, when adhesion is lost, by sliding friction. Development length provisions for plain bars for use in the assessment of existing structures have recently been established (Feldman et al. 2018) and show that development lengths between 1.4 and 1.53 times those required by deformed bars as calculated in accordance with Eq. 25.4.2.3a in ACI 2014 (ACI318 2014) are required for plain bars in the bottom cast position. An earlier work (Hassan & Feldman 2012) also suggests that splice specimens

reinforced with plain round bars cast in the bottom position are capable of resisting maximum loads that are 60% of those recorded for specimens reinforced with deformed bars.

A better understanding of the performance of plain hooked bars is therefore necessary to provide guidance to engineers responsible for the evaluation of historical structures. Such an experimental investigation has been initiated at the University of Saskatchewan, with the intent of establishing the capacity of hooked plain bars in comparison to that of modern deformed bars. Both 90 and 180° hooked bars are being evaluated. This paper describes the initial phase of this research, and includes a description of the specimen geometry, test setup and results.

2 EXPERIMENTAL PROGRAM

Figure 1(a) shows the overall geometry of the four beam-column specimens as included in the current investigation, and is similar to select specimens as tested by Marques and Jirsa (1975). Two of the specimens included 90° hooked bars, with the hooks in one specimen being plain reinforcement and those in the other being deformed bars, as shown in Figure 1(b). Figure 1(c) shows the geometry of the 180° hooked bars used in the other two specimens, again, with one specimen containing plain hooked bars and the other deformed hooked bars.

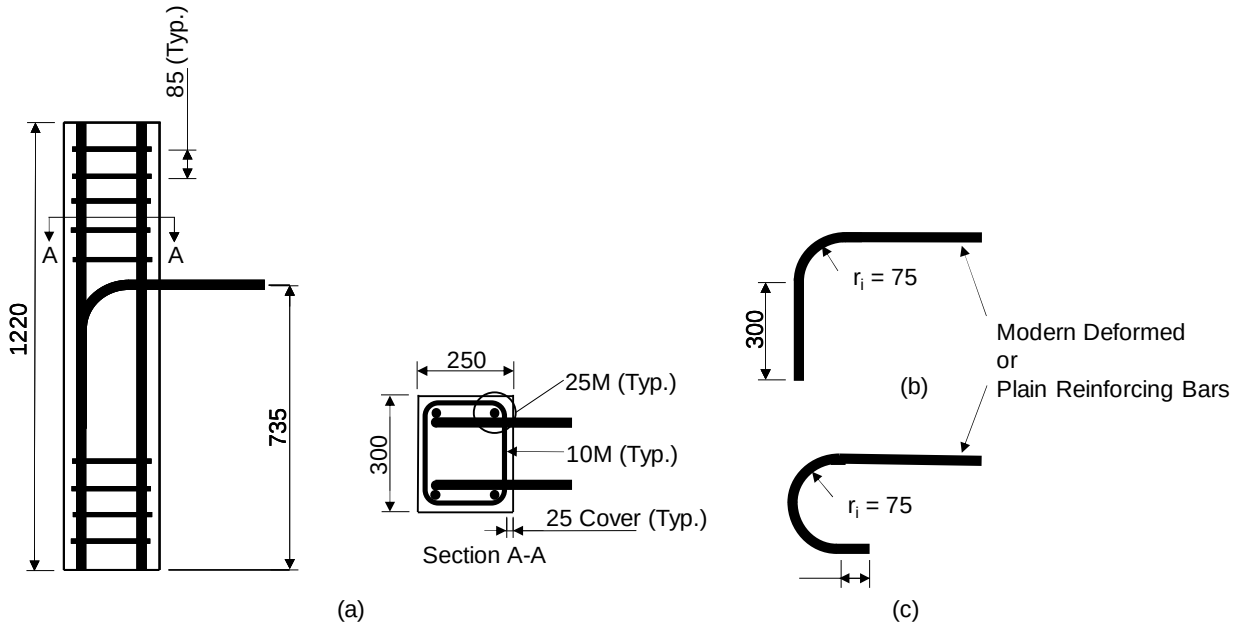

Figure 1: Geometry of the beam-column specimens: (a) elevation and cross-section, (b) details for 90° hooked bars, and (c) details for 180° hooked bars.

Section A-A in Figure 1(a) shows that all specimens had cross-sectional dimensions of 300 mm by 250 mm. The 300 mm specimen width ensured that a centre-to-centre spacing between the hooked bars was $6.2d_b$, where d_b is equal to the diameter of the hooked reinforcing bars, and so exceeded the $6d_b$ spacing necessary to ensure that group effect did not reduce the anchorage capacity of the hooked bars (Ajaam 2018). The specimen depth of 250 mm was reduced by 50 mm from that used by Marques and Jirsa (1975) to ensure that yielding of the Grade 300W plain hooked bars would not precede an anchorage failure.

Figure 2 shows that the testing setup used for the beam-column specimens was similar to that used by others (Marques & Jirsa 1975, Sperry et al. 2017a). Vertical threaded bars anchored to double-webbed wide flange structural steel sections at their top and bottom ends were tightened to ensure that a 200 kN

axial load (2.67 MPa axial stress) was applied to the specimen. While the magnitude of this axial load is different than that used by Sperry et al. (2017a) and Marques and Jirsa (1975), others (Marques and Jirsa 1975) have shown that that values of applied axial stress below 21 MPa resulted in negligible changes to the resulting tensile capacity of the hooked bars in beam-column specimens. Two Enerpac RCH-606 hollow plunger hydraulic cylinders mounted on the double-webbed plate girder reaction beam were used to apply the tensile load to the two hooked bars extending from each specimen. The lower front W310 x 74 beam served to simulate the compressive zone of the beam that would otherwise have been cast integrally with the column. The W310 x 74 top beam and double-webbed plate girder beam at the bottom left side of the specimen provided the necessary stabilizing support reactions. Two optoNCDT Micro-Epsilon laser displacement sensors were used to measure the slip of the hooked bars at a short distance away from the column face from which they extended. The hydraulic cylinders were then operated in force-control mode at a rate of 5 kN/min. with load and bar slip data logged at a rate of 100 Hz as testing progressed.

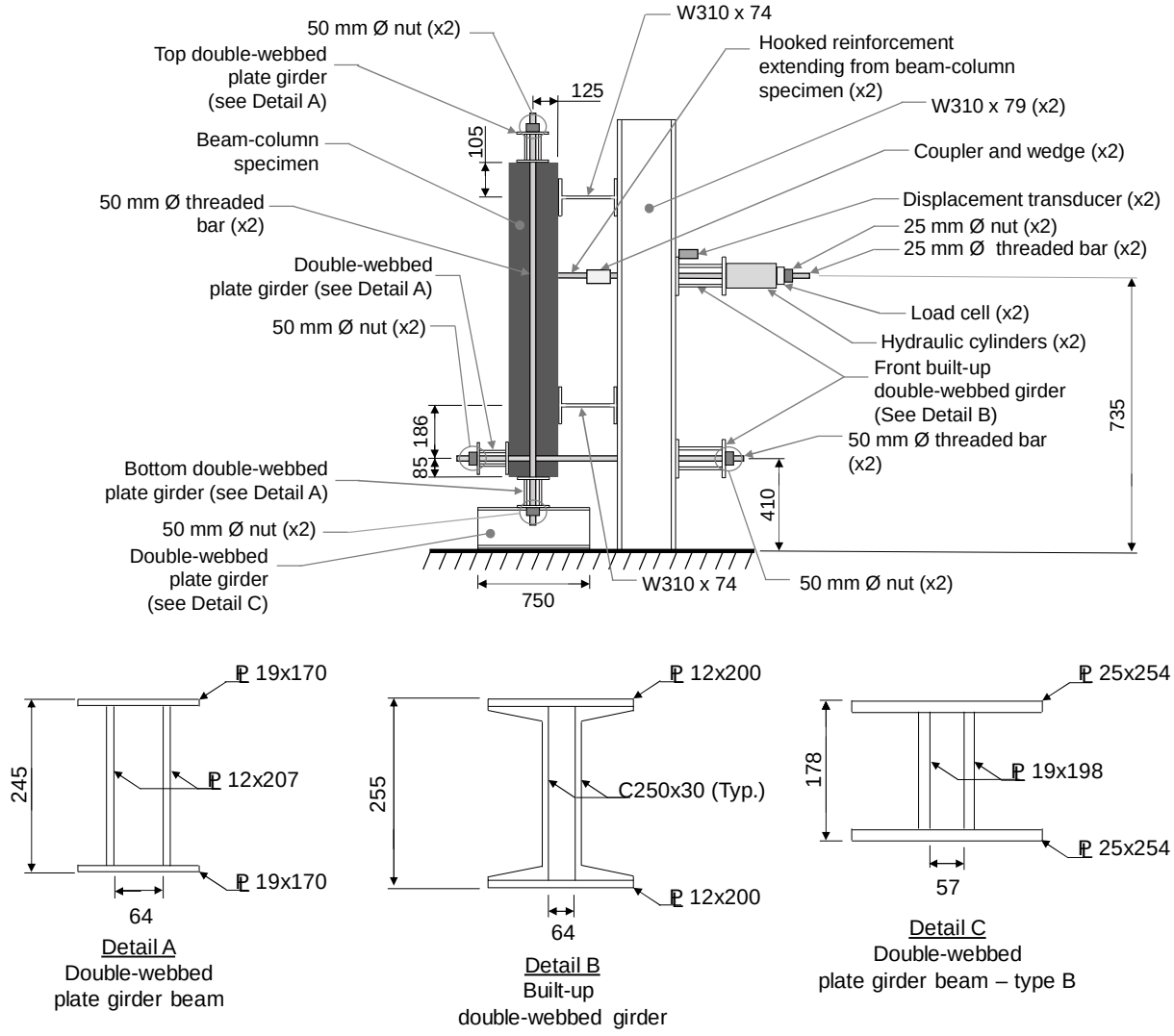

Figure 2: Test setup for the beam-column specimens

2.1 Concrete

Ready-mix concrete was used that included general use (Type GU) Portland cement. Air entrainment and admixtures were intentionally omitted from the mix, and a specified concrete compressive strength, f'_c, of 20 MPa was requested to match, as closely as possible, the historical concretes typical of the era in which plain reinforcement was used in construction (Feldman & Bartlett 2005). The mix design, per m^3 of concrete, was: 140 kg cement; 1242 kg crushed granite, carbonate, and gneiss coarse aggregate obtained from the Watrous pit in Saskatchewan; 937 kg of silica sand from Saskatchewan's Wakaw pit; and 78 kg of water. Coarse aggregate with a maximum size of 20 mm conformed to CAN/CSA A23.1-14 (2014a), and FA1 fine aggregate conformed to the requirements of the same standard.

The concrete compressive strength of each specimen was established at the time of testing, as reported in Table 1, from tests of three 100 mm diameter by 200 mm long concrete cylinders cast alongside the beam-column specimens. Specimens and cylinders were moist cured using wet burlap and plastic, respectively, for a seven day period following casting and were then allowed to cure in the laboratory environment until such time that they were tested.

2.2 Reinforcing Steel

Section A-A in Figure 1(a) shows that, in addition to the hooked bars used in select specimens, Grade 400W deformed reinforcing bars conforming to CAN/CSA G30.18 (CSA 2009) were used exclusively as the longitudinal and transverse reinforcement in the columns. All deformed reinforcement of each size was procured from a single heat, with excess lengths of the 25M bars used as the longitudinal reinforcement in the columns and as the test hooks used to establish their mechanical properties. The resulting static yield strength, f_{ys}, calculated in accordance with Rao et al. (1966) was 395 MPa, the dynamic yield strength, f_{yd}, was 419 MPa, the ultimate strength, f_u, was 649 MPa, and the modulus of elasticity, E, was 204 GPa.

Twenty five millimeter CAN/CSA G30.21 Grade 300W (CSA 2013) plain (i.e. undeformed) reinforcement was used as the test hooks in select specimens, with all material sourced from a single heat. These bars were blasted using silica sand at a blast pressure of 690 kPa and a nozzle distance of 250 mm to better simulate the surface roughness of historical bars (Feldman & Bartlett 2005). The roughness of the bars was quantified using a surface roughness tester to measure R_y, the distance between the highest peak and deepest valley within a single 0.25 mm stroke at ten locations on each bar. Table 1 shows that the resulting average value of R_y = 10.2 μm is a conservative representation of the surface roughness of historical reinforcement (Feldman & Bartlett 2005). The mechanical properties of these bars, as established from tests of excess bar lengths machined into coupons in accordance with ASTM A370 (ASTM 2014), were: f_{ys} = 328 MPa, f_{yd} = 355 MPa, f_u = 534 MPa, and E = 198 GPa.

Figure 1(a) shows that the closed ties that served as transverse reinforcement for the column were spaced at 85 mm on centre outside of the hook region. The decision to omit any transverse reinforcement within the hook region was done with consideration to test results reported by Marques and Jirsa (1975) as doing so would ensure an anchorage failure prior to yielding of the hooks.

3 Test Results and Analysis

Table 1 shows the test results for the four specimens, including: the resulting concrete compressive strength, f'_c; the measured surface roughness of the plain hooked bars as were included in Specimens 90P and 180P; the maximum obtained load for each hooked bar, P_{max}; and the slip at the maximum load level as measured for each hooked bar using the laser displacement transducers. Note that all reported values of maximum applied load have been normalized by the square root of the concrete compressive strength as has been shown to be reasonable for the development length of plain bars (Feldman & Bartlett 2005) and as used in provisions for the development and anchorage of deformed bars (CSA 2014b, ACI318 2014).

Table 1: Test Results

Specimen ID[a]	Bar	Age at test (days)	f'_c (MPa)	R_y (μm)	$P_{max}/\sqrt{f'_c}$ (kN/√MPa)	slip @ P_{max} (mm)
90P	A	49	6.35	10.1	16.7	9.30
	B			10.9	14.8	9.52
180P	A	54	6.63	9.91	17.3	6.34
	B			10.1	15.9	6.68
90D	A	48	10.2	n/a	23.8	13.5
	B				22.4	15.2
180D	A	44	9.91	n/a	23.5	11.5
	B				22.1	11.3

[a]Specimen identification consists of a number that correspond to the hook geometry (i.e. 90 or 180° bend) followed by a letter indicating whether the bar was plain (P) or deformed (D).

Table 1 shows that the as-tested values of the concrete compressive strength were significantly lower than the specified target strength. The concrete mix design used by others in this research stream (Hassan & Feldman 2012, Sekulovic MacLean 2014, Feldman et al. 2018) was altered by almost halving the cement content by weight since strengths as high as 35.8 MPa had been reported. It was further suspected that insufficient mixing of the concrete batch in the ready-mix truck may have resulted due to the small load. These issues will be evaluated and rectified moving forward. Nonetheless, segregation or any other problems that may have affected the performance of the concrete and so the capacity of the hooked bars was not evident.

Specimen cracking was monitored as testing progressed, with Figure 3 showing the crack pattern following testing for a representative specimen (Specimen 90P). Cracking of all specimens was first noted to initiate on the front face (Fig. 3(d)), as radial cracks developed around each hooked bar at an approximate load of $0.5P_{max}/\sqrt{f'_c}$. These cracks eventually lengthened, with those closest to the horizontal orientation reaching the side faces of the specimen. The cracks on the front face of the specimen likely resulted from a loss of adhesion between the straight length of the hooked bar and the surrounding concrete. Horizontal cracking tended to occur at the level of the straight length of the hooked bars on both side faces of each specimen (Figs. 3(a) and (c)), with vertical and diagonal cracks then extending from the initial horizontal crack, towards the front face of the specimen. Cracking on the back face (Fig. 3(b)) occurred later, at a load of approximately $0.75\ P_{max}/\sqrt{f'_c}$, and generally extended horizontally across the width of the specimen, with vertical cracking typically extending, as a minimum, along the vertical tail end or hook diameter, for 90 and 180° hooked bars, respectively. The progression of cracking and the resulting crack patterns were therefore similar to those reported by others (Sperry et al. 2017a). It also appeared that the normalized load at which cracks initiated, and the degree of cracking, was similar for specimens containing both plain and modern deformed hooked bars.

It was ultimately determined that the specimens containing 90° plain or modern deformed hooked bars failed due to side blowout, characterized by spalling of concrete from the side faces of the member that resulted in exposure of the hooked bars. A sizeable amount of concrete was then pulled forward with the hooked bars from the front specimen face. Specimens containing 180° hooked plain or modern deformed bars failed by front face blowout, and so displayed large amounts of concrete spalling quite suddenly from the front face of the specimen.

Table 1 shows that the resulting average normalized values of maximum applied load, $P_{max}/\sqrt{f'_c}$. for the two hooked bars in each specimen were 15.8 and 16.6 kN/√MPa for specimens containing 90 and 180° plain hooked bars, respectively; and 23.1 and 22.8 kN/√MPa for the specimens contained 90 and 180° modern deformed hooked bars, respectively. These results are consistent with those reported by others (Sperry et al. 2018) in that the anchorage strength of 90 and 180° hooks is similar. The results also show that the anchorage strength of plain hooked bars is about 30% less than the results obtained for modern deformed bars. The anchorage strength of hooked bars results from a combination of bond between the bar and the surrounding concrete and engagement of the concrete in front of the hook. In contrast, the capacity of lap

splices and development of straight bar lengths results from bond strength alone. Even though results are based on a very limited dataset, it therefore appears reasonable that anchorage strength of plain hooked bars is more similar to modern deformed hooked bars as shown herein, as compared to the capacity of lap splices as reported elsewhere (Hassan & Feldman 2012).

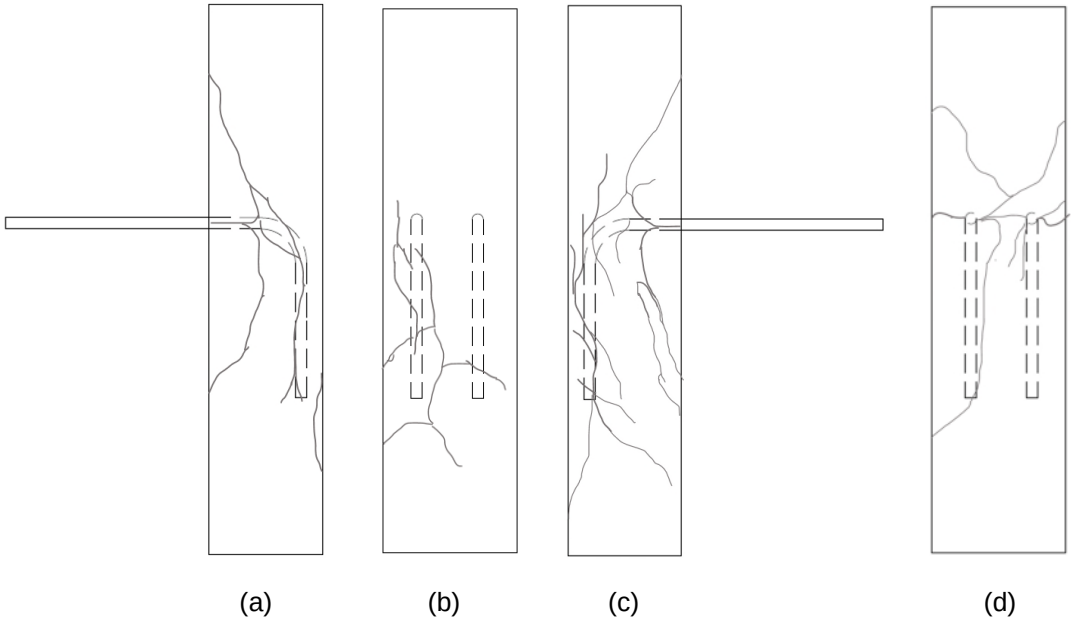

Figure 3: Crack pattern at failure for the specimen containing 90° hooked plain bars: (a) west side face, (b) back face, (c) east side face, and (d) front face.

Figures 4(a) and (b) show the normalized applied load versus bar slip as measured by the laser displacement transducers for the 90 and 180° hooked bars, respectively. In both cases, slip associated with the normalized maximum load is larger for the modern deformed hooked bars as compared to the plain hooked bars. Figure 4(a) also shows that slip at the normalized failure load is greater for the modern deformed hooked bars as compared to the plain hooked bars, while it is evident from Figure 4(b) that slip data following the maximum normalized load were not measured for the 180° plain hooked bars as a result of a malfunction of the laser displacement transducers during the testing of this beam-column specimen. The radial stresses caused by the ribs on the modern deformed bars results in localized crushing of the adjacent concrete, and so is believed to result in the increased slip as noted for these bars as shown in Figures 4(a) and (b). Data reported in Table 1 also shows that slip at the maximum normalized load level is 44 and 26% greater for 90° hooked plain and modern deformed bars, respectively, as compared to 180° hooked bars.

Results as presented herein are based on a limited test database of beam-column specimens. Each specimen as reported contained a unique combination of bar type and hook geometry. Experimental work is therefore ongoing and will add five replicates of each specimen type describe in this paper to the test database, thus allowing for statistical comparisons of the quantifiable information as contained in this paper to be made. The extended test database will therefore provide confirmation of the existence of any statistical difference in the capacity of 90 and 180° hooked plain bars, and in the capacity of plain and modern deformed bars of the two hook geometries.

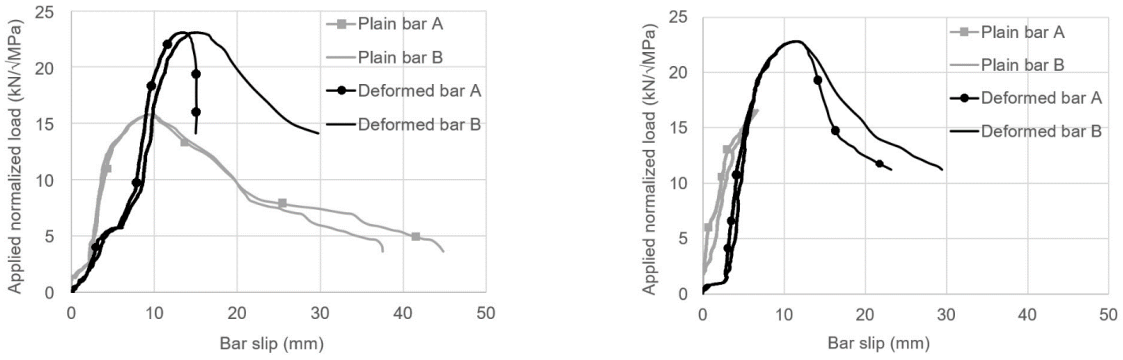

(a) (b)

Figure 4: Normalized applied load versus bar slip: (a) 90° plain and modern deformed hooked bars, and (b) 180° plan and modern deformed hooked bars.

SUMMARY AND CONCLUSIONS

This paper describes a preliminary experimental program, consisting of beam-column specimens, used to evaluate the performance of hooked plain reinforcing bars in relation to modern deformed bars in concrete. A total of four specimens were included, with the hook geometry (90 or 180°), and bar type (plain or modern deformed) differing in each of the specimens. All specimens were 300 mm wide by 250 mm deep by 1220 mm tall. The centre-to-centre spacing between the 25 mm diameter hooked bars was therefore equal to 6.2 times the bar diameter and so ensured that group effect did not influence the capacity of the hooked bars. The following significant observations and conclusions were noted:

1. A review of cracking as testing progressed revealed that the extent of cracking and magnitude of the normalized applied load at which cracking initiated was similar for specimens containing either plain or modern deformed hooked bars. Specimens containing 90° hooked bars failed due to side blowout followed by front face failure, whereas a front face blowout occurred for specimens containing 180° hooked bars.

2. The anchorage capacity of 90 and 180° hooks for either bar type were similar; however, the anchorage capacity of plain hooked bars was about 30% less than that measured for the modern deformed bars. This margin appears to be slightly less than that reported for lap splice lengths and is likely attributed to the capacity of hooked bars resulting from a combination of bond between the bar and the surrounding concrete and the engagement of the concrete in front of the hook. The latter mechanism is not available for lap spliced bars.

3. Bar slip associated with both the normalized maximum and residual loads is greater for hooked modern deformed bars in comparison to the plain bars. It is expected that the localized crushing of concrete in advance of the ribs on the deformed bars results in this increased slip.

ACKNOWLEDGEMENTS

Financial support for this project was provided by the second author's NSERC Discovery Grant and funds provided by the Saskatchewan Centre for Excellence in Transportation and Infrastructure (SCETI). Lafarge Canada Inc. additionally provided the ready-mix concrete, and SSAB provided, in-kind, steel required for the fabrication of select test frame components. The authors gratefully acknowledge the assistance of Brennan Pokoyoway, Structures Laboratory Technician, undergraduate research assistants Owen Beach

and Amy Miller, and former graduate student Shailza Singh, for assistance with the preparation and testing of specimens.

REFERENCES

ACI Committee 318. 2014. *318-14: Building Code Requirements for Structural Concrete and Commentary*, American Concrete Institute, Farmington Hills, MI.

Ajaam, A., Yasso, S., Darwin, D., O'Reilly, M., Sperry, J. Anchorage Strength of Closely Spaced Hooked Bars. *ACI Structural Journal*, *76*, 115(4): 1143 – 1152.

ASTM. 2014. *ASTM A370-14 – Standard Test Method and Definitions for Mechanical Testing of Steel Products*, ASTM International, West Conshohocken, PA.

Cleland, D.J., Cummings, S.J., Rankin, G.I., Taylor, S., Scott, R.H. 2001. Influence of Reinforcement Anchorage on the Bending and Shear Capacity of Bridge Decks. *The Structural Engineer*, 79(16): 24 – 31.

CSA. 2009. *CSA G30.18-09 – Carbon Steel Bars for Concrete Reinforcement*, Canadian Standards Association, Mississauga, ON.

CSA. 2013. *CSA G40.20-13/G40-21-13 (R2018) General Requirements for Rolled or Welded Structural Quality Steel/Structural Quality Steel*, Canadian Standards Association, Mississauga, ON.

CSA. 2014a. *CAN/CSA A23.1/A23.2-14 Concrete Materials and Concrete Construction/Test Methods and Standard Practices for Concrete*, Canadian Standards Association, Mississauga, ON.

CSA. 2014b. *CAN/CSA A23.3 Design of Concrete Structures*, Canadian Standards Association, Mississauga, ON.

Feldman, L.R., Bartlett, F.M. 2005. Bond Strength Variability in Pullout Specimens with Plain Reinforcement. *ACI Structural Journal*, 102(6): 860 – 867.

Feldman, L.R., Poudyal, U., Cairns, J. Proposed Development Length Equations for Plain Bars. *ACI Structural Journal*, 115(6): 1615 – 1623.

Hassan, M.N., Feldman, L.R. 2012. Behavior of Lap Spliced Plain Steel Bars. *ACI Structural Journal*, 109(2): 235 – 244.

Marques, J.L., Jirsa, J.O. 1975. A Study of Hooked Bar Anchorages in Beam-Column Joints. *ACI Journal Proceedings*, 72(5): 198 – 209.

Minor, J., Jirsa, J.O. 1975. Behavior of Bent Bar Anchorages. *ACI Journal Proceedings*, 72(4): 141 – 149.

Mylrea, T.D. 1934. The Carrying Capacity of Semicircular Hooks. *Journal of the American Concrete Institute*, 24: 240 – 263.

Pinc, R., Watkins, M., Jirsa, J.O. 1977. The Strength of Hooked Bar Anchorages in Beam-Column Joints. *CESRL Report No. 77-3, Department of Civil Engineering – Structures Research Laboratory*, University of Texas at Austin, Austin, TX, 67 pp.

Rao, N.R.M., Lohrmann, M., Tall, L. 1966. Effects of Strain Rate on the Yield Stress of Structural Steels. *ASTM Journal of Materials*, 1(1): 241 – 262.

Sekulovic MacLean, M., Feldman, L.R. 2014. Effects of Casting Position and Bar Shape on Bond of Plain Bars. *ACI Structural Journal*, 111(2): 323 – 330.

Sperry, J., Yasso, S., Searle, N., DeRubeis, M., Darwin D., O'Reilly, M., Matamoros, A., Feldman, L.R., Lepage, A., Lequesne, R.D., Ajaam, A. 2017a. Conventional and High-Strength Hooked Bars – Part 1: Anchorage Tests. *ACI Structural Journal*, 114(1): 255 – 265.

Sperry, J., Darwin. D., O'Reilly, M., Lequesne, R.D., Yasso, S., Matamoros, A., Feldman, L.R., Lepage, A. 2017b. Conventional and High-Strength Hooked Bars – Part 2: Data Analysis. *ACI Structural Journal*, 114(1): 267 – 276.

Sperry, J., Darwin, D., O'Reilly, M., Lepage, A., Lequesne, R.D., Matamoros, A., Feldman, L.R., Yasso, S., Searle, N., DeRubeis, M., Ajaam, A. 2018. Conventional and High-Strength Hooked Bars – Part 3: Detailing Effects. *ACI Structural Journal*, 115(1): 247 – 257.